

3D Printing of Photocurable Resin Reinforced by Functionalised Graphene Nanoplatelets [†]

Mohamad Alsaadi ^{1,2,3,*} , Eoin P. Hinchy ^{1,4} , Conor T. McCarthy ^{1,4}, Vicente F. Moritz ² , Alexandre Portela ²
and Declan M. Devine ^{2,*} 

¹ CONFIRM Centre for Smart Manufacturing, University of Limerick, V94 T9PX Limerick, Ireland; eoin.hinchy@ul.ie (E.P.H.); conor.mccarthy@ul.ie (C.T.M.)

² PRISM Research Institute, Technological University of the Shannon, Dublin Rd, N37 HD68 Athlone, Ireland; a00288528@student.ait.ie (V.F.M.); alexandre.portela@ait.ie (A.P.)

³ Materials Engineering Department, University of Technology, Baghdad 10066, Iraq

⁴ School of Engineering, University of Limerick, V94 T9PX Limerick, Ireland

* Correspondence: mohamad.alsaadi@ait.ie (M.A.); declan.devine@tus.ie (D.M.D.)

[†] Presented at the 4th International Online Conference on Nanomaterials, 5–19 May 2023; Available online: <https://iocn2023.sciforum.net/>.

Abstract: The influence of functionalised graphene nanoplatelets with melamine on the thermal and mechanical properties of a 3D-printed photopolymerisable resin is investigated. In this work, a liquid-based 3D printer and stereolithography were employed to fabricate the 3D-printed parts, and a commercial dimethacrylate-based resin was used. The 3D-printed parts were subjected to ultraviolet and thermal post-curing stages to improve thermal and mechanical behaviour. The quality of the graphene nanoplatelets' functionalisation was characterised by Fourier transform infrared spectroscopy and thermogravimetric analysis. Thermal and mechanical characterisations were performed via thermogravimetric, tensile, and Izod impact tests. The fractured surfaces were observed via scanning electron microscopy. The degree of graphene nanoplatelet dispersion in the polymer matrix is enhanced by bonding with melamine via π - π interactions and inhibited surface defect formation. Results show property enhancements of up to 35% in tensile strength, 78% in impact strength, and 38% in residual weight at 400 °C.

Keywords: 3D printing; polymer nanocomposites; stereolithography; functionalisation; graphene nanoplatelets; thermal properties; mechanical properties



Citation: Alsaadi, M.; Hinchy, E.P.; McCarthy, C.T.; Moritz, V.F.; Portela, A.; Devine, D.M. 3D Printing of Photocurable Resin Reinforced by Functionalised Graphene Nanoplatelets. *Mater. Proc.* **2023**, *14*, 20. <https://doi.org/10.3390/IOC2023-14540>

Academic Editor: Ullrich Scherf

Published: 5 May 2023



Copyright: © 2023 by the authors. Licensee MDPI, Basel, Switzerland. This article is an open access article distributed under the terms and conditions of the Creative Commons Attribution (CC BY) license (<https://creativecommons.org/licenses/by/4.0/>).

1. Introduction

The need for complex geometric designs provided with good mechanical and thermal properties suitable for manufacturing through 3D printing fabrication methods has offered opportunities to develop novel leading manufacturing technologies. SLA technology fabricates 3D prototypes, patterns, and parts layer-by-layer by focusing an ultraviolet (UV) laser beam on a liquid photopolymerisable resin to crosslink the molecule chains [1–3]. However, using stereolithography (SLA) is not always appropriate for manufacturing advanced parts mainly because of insufficient mechanical properties and poor thermal characteristics [4,5].

Recent studies have employed nanofillers as an effective technique to develop photocurable resins for liquid-based 3D printers, enabling the final properties to improve considerably by incorporating small contents of a nanofiller. For instance, Mu et al. used digital light processing 3D printing to investigate the tensile properties of a photocurable acrylic-based resin by adding multiwalled carbon nanotubes in contents of 0.1 to 0.6 wt% [6]. Furthermore, Idowu et al. [7] fabricated graphene nanoplatelets (GNP) reinforced epoxy-based nanocomposites using direct ink writing (DIW) to study their mechanical and

damping characteristics. The authors concluded that a GNP addition of 0.1 wt% improved tensile strength by 17%.

Several parameters should be controlled when using nanofillers in photopolymerisation techniques. For example, at elevated particle loading levels, the resin viscosity becomes high enough to hinder the mixing, leading to an increased curing time [4]. In addition, low interfacial adhesion due to poor dispersibility and nanoparticle aggregations acts as a stress concentration defect [8]. Covalent functionalisation is carried out by the oxidation of GNP in acidic media to improve the interfacial adhesion between nanoparticles and a polymer matrix via direct chemical bonding [9,10]. On the other hand, noncovalent functionalisation is used to modify the GNP surface, which is characterised by interactions between delocalised π bonds on the nanoparticle's surface and hexagonal ring structures on the functionalising moieties [10,11]. Moreover, noncovalent functionalisation has the essential advantage that it neither destroys the surface of the nanomaterial nor affects its final structure [12].

Based on the literature surveyed, the mechanical and thermal characteristics of various nanoparticle-reinforced 3D-printed (3DP) composites have been investigated. To the best of found knowledge, researchers in these studies did not inspect the effect of melamine-GNP (M-GNP) on these properties of 3DP nanocomposites. In this work, a photocurable resin for SLA 3D printing is used to produce dimethacrylate-based GNP nanocomposites functionalised with melamine, which has hexagonal rings suitable for π - π interactions to generate M-GNP using a non-destructive shaking and ball-milling process. Melamine has a coupled structure that contains hybridised carbon, making it appropriate for noncovalent functionalisation through π - π interactions. The tensile strength, impact resistance, and thermal degradation were investigated. The fracture surface morphology was observed via scanning electron microscopy (SEM).

2. Materials and Methods

2.1. Material

The photocurable polymer used in this study is a commercial Clear V4 resin (FormLabs Inc., Somerville, MA, USA), containing a mixture of 55–75% urethane dimethacrylate (UDMA), 15–25% methacrylate monomers, and <0.09% diphenyl (2,4,6 trimethylbenzoyl) phosphine oxide (BAPO) as a photoinitiator. Clear (neat) resin is a leading, standard FormLabs resin, being a rigid material claimed to suit designing, mould-making, and microfluidic channels. This resin is suited for rapid prototyping, functional testing, and product development. The GNP is used as reinforcement with a particle size of 5 μm , surface area of 50–80 $\text{m}^2\cdot\text{g}^{-1}$, and thickness of 15 nm. Melamine was used to functionalise GNP, and N,N-dimethylformamide (DMF) to dissolve melamine and GNP. These materials were supplied from Sigma-Aldrich (Gillingham, UK).

2.2. Preparation of Functionalised M-GNP

Melamine (250 mg) was dissolved in 75 mL of DMF by stirring for 15 min. Then, GNP (250 mg) was added, and the mixture was ultrasonicated for 15 min. For functionalisation, the resulting solution was shaken and ball-milled for 24 h (Figure 1a). Melamine was bound by π - π interactions with GNP (Figure 1b). The hexagonal rings of melamine were adsorbed onto the surface of GNP. Then, the mixture was vacuum-filtered for 45 min. The retained black solid particles were vacuum-dried at room temperature.

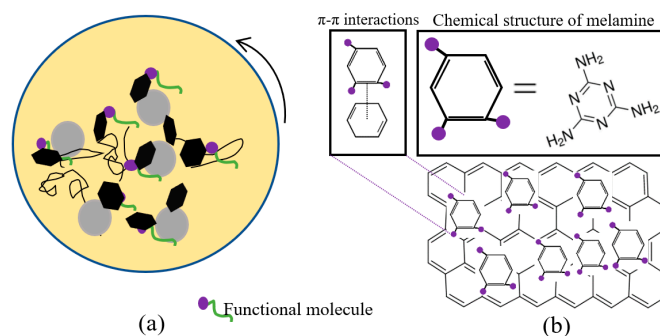


Figure 1. Functionalisation process of GNPs: (a) Schematic illustration of shaking and ball-milling process and functional molecules. (b) Schematic illustration of the functionalisation of GNP with melamine.

2.3. Preparation of M-GNP Nanocomposite Resin

Functionalised M-GNP was added to the photocurable resin after increasing its temperature to 40 °C to decrease resin viscosity and enhance M-GNP dispersion. The mixture was stirred in a planetary centrifugal mixer (Thinky Mixer ARM-310 CE, THINKY Co. Oxfordshire, UK) at 1500 rpm for 30 min. This mixer uses an efficient mechanism where the jar containing the solution revolves clockwise, and the jar itself is rotated counterclockwise to generate shear force, assisting in obtaining a homogeneous resin. Finally, the resin mixture was stirred at 200 rpm under a vacuum of 0.1 bar for 30 min to remove air bubbles. This photocurable resin was added to the vat of a Form 2 SLA 3D printer (FormLabs Inc., Somerville, MA, USA) to produce the 3DP components.

2.4. Fabrication of 3D-Printed Samples

The 3D printing process was carried out using Form 2 SLA with a layer thickness of 0.05 mm under a 250 mW UV laser (405 nm wavelength). The 3DP samples were washed with isopropyl alcohol (IPA) for 30 s in two stages after removing the support structure. Then, pressurised air was used to dry the samples to avoid the IPA damaging the still-sensitive components. The printed samples were post-cured in two stages, firstly under UV light of 1.25 mW·cm⁻² for 60 min and then in an induction oven at 60 °C for another 60 min.

2.5. Characterisations and Tests

The chemical compound of the M-GNP was characterised by Fourier transform infrared spectroscopy (FTIR) (ATR-FTIR, Perkin Elmer Spectrum, Waltham, MA, United States) and thermogravimetric analysis (Pyris 1 TGA, Perkin Elmer, Waltham, MA, United States). TGA was used to determine the thermal degradation behaviour of the pristine GNP, melamine, and M-GNP 3D from 25 to 1000 °C at a ramp rate of 10 °C·min⁻¹; this was also used for the 3DP samples with the same procedure and the final temperature was 600 °C in nitrogen atmosphere. The tensile testing was performed based on ASTM D638 with type V specimens (gauge length 7.62 mm) using a Zwick Roll machine (Z010, GmbH & Co. KG, Baden-Wurttemberg, Germany) with a loadcell capacity of 10 kN and a crosshead speed of 1 mm/min. The fracture surfaces of the tensile samples were later observed by a Mira SEM (Tescan, Oxford Instruments, Cambridge, UK) to evaluate the dispersion quality of the GNP. An impact test was carried out by the Izod impact machine equipped with a 5.5 J Hammer (Instron CEAST Norwood, MA, United States) based on ASTM D4812 for unnotched samples. At least three samples were tested for each experiment.

3. Results and Discussion

3.1. Characterisation of M-GNP Behaviour

GNP functionalisation is verified by spectroscopic analysis. The FTIR spectra of melamine, pristine GNP, and melamine-GNP are shown in Figure 2. The melamine and the

functionalised M-GNP spectrum displayed significant signals, at about 1620 and 3310 cm^{-1} , which indicated the presence of N–H bonds. In addition, peaks of C–O stretching and C=C stretching of the pristine GNP were located on the M-GNP at 1590 and 1075 cm^{-1} . These peaks confirmed the functionalisation of the GNP surface by the low-energy ball-milling process [10,11,13,14]. Furthermore, a stretched broad peak appeared at about 3090 cm^{-1} , as O–H bonds in chemically modified M-GNP were generated from the mechanochemical ball-milling and shaking process [11].

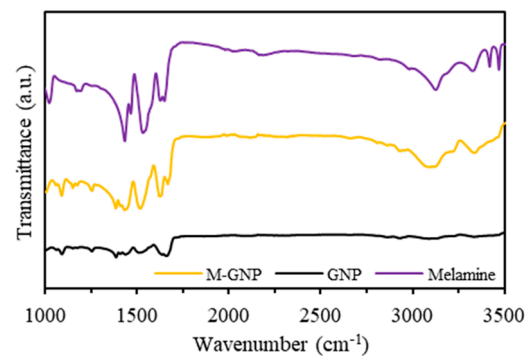


Figure 2. FTIR spectra of melamine, GNP, and M-GNP.

TGA analysis (Figure 3) also confirmed the noncovalent functionalisation of M-GNP. The degradation behaviour of M-GNP is understood as a combination of neat melamine and GNP. M-GNP revealed a high thermal degradation of melamine after 250 $^{\circ}\text{C}$. The degradation decreased slightly between 300 $^{\circ}\text{C}$ and 700 $^{\circ}\text{C}$, which was like the carbonisation noticed for GNP. M-GNP decomposition was around 50% between 300 and 700 $^{\circ}\text{C}$, serving as evidence of functionalisation.

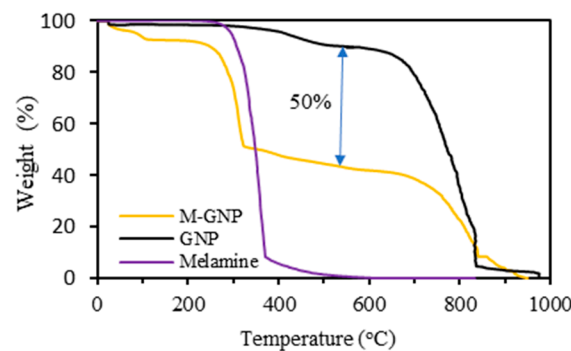


Figure 3. TGA curves of the melamine, GNP and M-GNP.

3.2. Thermal and Mechanical Properties of the M-GNP Nanocomposites

The thermal stability of the 3DPM-GNP nanocomposites was investigated via TGA. Figure 4 displays the TGA curves of M-GNP nanocomposites. Neat sample began to lose weight before M-GNP nanocomposites. Table 1 lists the decomposition temperatures for the weight loss of 5 wt% and the residual weight at 400 $^{\circ}\text{C}$, designated as T_5 and W_{400} , respectively. These results indicate that the incorporation of M-GNP considerably enhances the thermal stability of the polymer matrix. The T_5 of the nanocomposite containing 0.1 wt% M-GNP was 304 $^{\circ}\text{C}$ with 29% greater than that of the neat one. Similarly, the residual weight at 400 $^{\circ}\text{C}$ was 77 wt%, while for the pure material, this value was 56 wt%, an increment of 38% for the 0.1 wt% M-GNP nanocomposite. The improvement in thermal stability with such a small amount of M-GNP was owing to the good interfacial adhesion between M-GNP and the 3D-printed polymer matrix since the noncovalent functionalisation of melamine via π - π interactions improved the dispersion of the GNP, which also enhanced the UV curing reaction with the dimethacrylate-based photocurable resin [14].

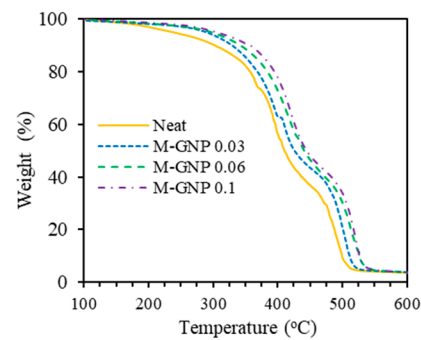


Figure 4. Weight loss versus temperature.

Table 1. TGA values of the M-GNP nanocomposites.

Material	T_5 (°C)	W_{400} (%)
Neat	56	236
M-GNP 0.03	63	288
M-GNP 0.06	72	296
M-GNP 0.1	77	304

The tensile and impact properties of the 3DP parts are shown in Figure 5. The tensile strength and impact resistance values were increased with increasing content of M-GNP; hence, with the incorporation of 0.1 wt% of M-GNP, the tensile strength and impact resistance reached their maxima. For instance, compared with the neat material, the tensile strength and impact resistance of the 0.1 wt% M-GNP nanocomposite were improved by 35% and 78%, respectively.

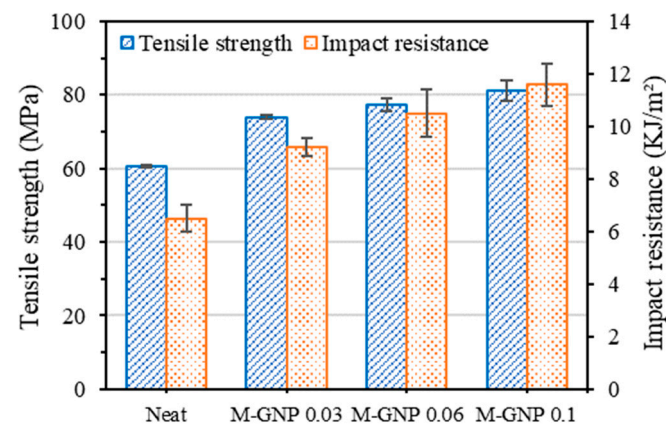


Figure 5. Tensile strength and impact resistance.

Figure 6 displays the SEM fracture surface morphology of the neat and nanocomposite samples. M-GNP agglomerations are not observed in the resin matrix. The M-GNP nanoparticles were embedded and homogeneously dispersed within the matrix. This indicates that melamine inhibits the GNP from aggregating through π - π interactions between the surfaces of GNP. Furthermore, the melamine's amino groups (-NH₂) likely bonded covalently and led to strong interfacial interactions with the polymer matrix system. These interactions resulted in improved load transfer across the interface between the matrix and nanoparticle within the polymer nanocomposite [10]. Thus, the larger specific surface area of the multilayer M-GNP resulted in greater strength for the nanocomposites.

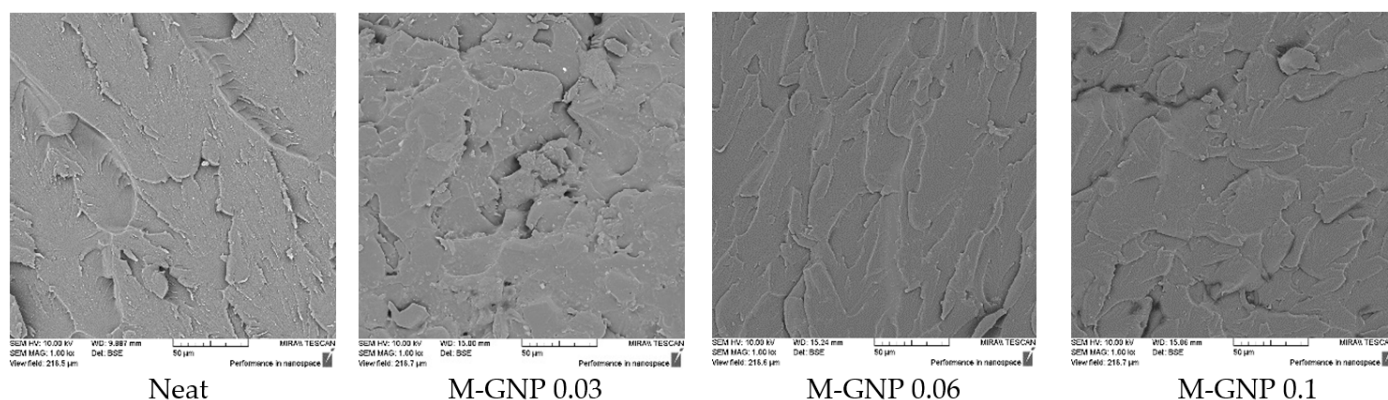


Figure 6. SEM micrographs of the tensile fracture surface.

4. Conclusions

The effects of GNP functionalised with melamine on the tensile and impact properties of the 3DP-photoresin nanocomposites were examined. The functionalisation of the GNP was proved via FTIR and TGA. The improvement in thermal stability, tensile, and impact properties with such a small amount of M-GNP is owing to the strong interfacial adhesion between M-GNP and the 3DP polymer matrix since the noncovalent functionalisation with melamine via π - π interactions improved GNP dispersion and inhibited surface defect formation, as well as enhancing the UV curing reaction of the dimethacrylate-based photocurable resin. Results exhibited enhancements of up to 35% in tensile strength, 78% in impact strength, and 38% in residual weight at 400 °C.

Author Contributions: Conceptualisation, M.A.; methodology, M.A. and D.M.D.; resources, M.A., D.M.D., C.T.M., E.P.H., V.F.M., and A.P.; writing—original draft preparation, M.A.; writing—review and editing, M.A., E.P.H., V.F.M., A.P., and D.M.D.; visualisation, M.A.; supervision, C.T.M., E.P.H., and D.M.D.; project administration, D.M.D.; funding acquisition, M.A., C.T.M., and D.M.D. All authors have read and agreed to the published version of the manuscript.

Funding: This research project is funded by Marie Skłodowska-Curie grant agreement No. 847577 cofunded by the European Regional Development Fund and Science Foundation Ireland (SFI) under Grant Number SFI/16/RC/3918 (Smart Manufacturing, Confirm Centre, UL).

Institutional Review Board Statement: Not applicable.

Informed Consent Statement: Not applicable.

Data Availability Statement: The data presented in this study are available on request from the corresponding author.

Conflicts of Interest: The authors declare no conflict of interest.

References

- Melchels, F.P.W.; Feijen, J.; Grijpma, D.W. A Review on Stereolithography and Its Applications in Biomedical Engineering. *Biomaterials* **2010**, *31*, 6121–6130. [[CrossRef](#)] [[PubMed](#)]
- Alsaadi, M.; Hinchy, E.P.; McCarthy, C.T.; Moritz, V.F.; Zhuo, S.; Fuenmayor, E.; Devine, D.M. Liquid-Based 4D Printing of Shape Memory Nanocomposites: A Review. *J. Manuf. Mater. Process.* **2023**, *7*, 35. [[CrossRef](#)]
- Li, X.; Yu, R.; He, Y.; Zhang, Y.; Yang, X.; Zhao, X.; Huang, W. Four-Dimensional Printing of Shape Memory Polyurethanes with High Strength and Recyclability Based on Diels-Alder Chemistry. *Polymer* **2020**, *200*, 122532. [[CrossRef](#)]
- Li, J.; Wang, L.; Dai, L.; Zhong, L.; Liu, B.; Ren, J.; Xu, Y. Synthesis and Characterization of Reinforced Acrylate Photosensitive Resin by 2-Hydroxyethyl Methacrylate-Functionalized Graphene Nanosheets for 3D Printing. *J. Mater. Sci.* **2018**, *53*, 1874–1886. [[CrossRef](#)]
- Borra, N.D.; Neigapula, V.S.N. Parametric Optimization for Dimensional Correctness of 3D Printed Part Using Masked Stereolithography: Taguchi Method. *Rapid Prototyp. J.* **2023**, *29*, 166–184. [[CrossRef](#)]
- Mu, Q.; Wang, L.; Dunn, C.K.; Kuang, X.; Duan, F.; Zhang, Z.; Qi, H.J.; Wang, T. Digital Light Processing 3D Printing of Conductive Complex Structures. *Addit. Manuf.* **2017**, *18*, 74–83. [[CrossRef](#)]

7. Idowu, A.; Thomas, T.; Boesl, B.; Agarwal, A. Cryo-Assisted Extrusion 3D Printing of Shape Memory Polymer-Graphene Composites. *J. Manuf. Sci. Eng.* **2023**, *145*, 041003. [[CrossRef](#)]
8. Alsaadi, M.; Younus, B.; Erklig, A.; Bulut, M.; Bozkurt, O.; Sulaiman, B. Effect of Graphene Nano-Platelets on Mechanical and Impact Characteristics of Carbon/Kevlar Reinforced Epoxy Hybrid Nanocomposites. *Proc. Inst. Mech. Eng. Part C J. Mech. Eng. Sci.* **2021**, *235*, 7139–7151. [[CrossRef](#)]
9. Liu, L.; Etika, K.C.; Liao, K.-S.; Hess, L.A.; Bergbreiter, D.E.; Grunlan, J.C. Comparison of Covalently and Noncovalently Functionalized Carbon Nanotubes in Epoxy. *Macromol. Rapid Commun.* **2009**, *30*, 627–632. [[CrossRef](#)] [[PubMed](#)]
10. Cha, J.; Kim, J.; Ryu, S.; Hong, S.H. Comparison to Mechanical Properties of Epoxy Nanocomposites Reinforced by Functionalized Carbon Nanotubes and Graphene Nanoplatelets. *Compos. Part B Eng.* **2019**, *162*, 283–288. [[CrossRef](#)]
11. Kim, J.; Cha, J.; Chung, B.; Ryu, S.; Hong, S.H. Fabrication and Mechanical Properties of Carbon Fiber/Epoxy Nanocomposites Containing High Loadings of Noncovalently Functionalized Graphene Nanoplatelets. *Compos. Sci. Technol.* **2020**, *192*, 108101. [[CrossRef](#)]
12. Kim, J.; Cha, J.; Jun, G.H.; Yoo, S.C.; Ryu, S.; Hong, S.H. Fabrication of Graphene Nanoplatelet/Epoxy Nanocomposites for Lightweight and High-Strength Structural Applications. *Part. Part. Syst. Character.* **2018**, *35*, 1700412. [[CrossRef](#)]
13. Choi, E.-Y.; Han, T.H.; Hong, J.; Kim, J.E.; Lee, S.H.; Kim, H.W.; Kim, S.O. Noncovalent Functionalization of Graphene with End-Functional Polymers. *J. Mater. Chem.* **2010**, *20*, 1907. [[CrossRef](#)]
14. Wu, S.; Shi, T.; Zhang, L. Preparation and Properties of Amine-Functionalized Reduced Graphene Oxide/Waterborne Polyurethane Nanocomposites. *High Perform. Polym.* **2016**, *28*, 453–465. [[CrossRef](#)]

Disclaimer/Publisher's Note: The statements, opinions and data contained in all publications are solely those of the individual author(s) and contributor(s) and not of MDPI and/or the editor(s). MDPI and/or the editor(s) disclaim responsibility for any injury to people or property resulting from any ideas, methods, instructions or products referred to in the content.